Towards inverse design of biomimetic nanostructures exhibiting composite structural coloration

Bianca C. Datta, Sundeep K. Jolly, V. Michael Bove

Bianca C. Datta, Sundeep K. Jolly, V. Michael Bove, "Towards inverse design of biomimetic nanostructures exhibiting composite structural coloration," Proc. SPIE 10930, Advanced Fabrication Technologies for Micro/Nano Optics and Photonics XII, 1093012 (4 March 2019); doi: 10.1117/12.2510027

SPIE.

Event: SPIE OPTO, 2019, San Francisco, California, United States

Towards inverse design of biomimetic nanostructures exhibiting composite structural coloration

Bianca C. Datta[a], Sundeep K. Jolly[a], and V. Michael Bove, Jr.[a]

[a]MIT Media Lab, Massachusetts Institute of Technology, Cambridge, MA, United States

ABSTRACT

Structural color phenomena exhibited by several organisms result from interference and diffraction of light incident upon multilayer nanostructures. These biomimetic nanostructured surfaces produce structural coloration for desired angle-variant distributions of reflectance spectra. Previous work has demonstrated the utility of inverse design methodologies in the computational formulation of nanostructures tailored for specific spectral responses, generally tailored around a single spectral band. In this work, we depict a design methodology based around computational inverse design for the formulation of nanostructures exhibiting composite structural coloration in a variety of disjoint spectral bands. We furthermore depict example design constraints and study convergence with respect to the design trade space.

Such complex biological systems require advanced fabrication techniques, and replication of nanoscale features of this complexity has been difficult. Our designs are constrained for realizable fabrication using direct laser writing techniques such as two-photon polymerization. This process provides a toolkit with which to examine and build other bio-inspired, tunable, and responsive photonic systems and expand the range of achievable structural colors. Sample experimental results of nanostructures fabricated via two-photon polymerization are presented.

Keywords: biomimetics, two-photon polymerization, structural color, direct laser writing, inverse design

1. INTRODUCTION AND MOTIVATION

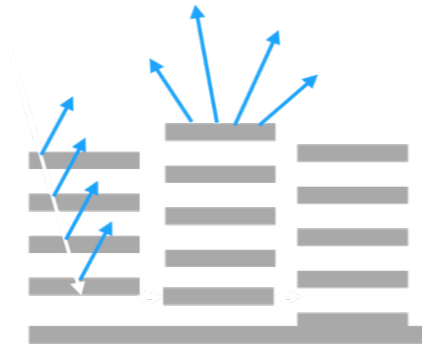

Figure 1. Generation of structural color in *Morpho* butterflies relies on the following phenomena: 1) Alternating layers of high and low index leads to constructive interference for blue coloration 2) Narrow shelf width leads to wide angular spread 3) Randomness in shelf height leads to rainbow suppression 4) Narrow gap between shelves leads to high reflectivity 5) Anisotropy in the vertical direction limits the angular range of reflectivity.[1]

Structural color phenomena found in nature produce compelling and vibrant visual displays resulting from interference and diffraction effects. The wings of the *Morpho* butterfly are a well-studied example of a biological system exhibiting structural coloration and a high degree of wide-angle iridescence due to a non-negligible

Corresponding author: E-mail: bdatta@mit.edu

Advanced Fabrication Technologies for Micro/Nano Optics and Photonics XII, edited by Georg von Freymann, Winston V. Schoenfeld, Raymond C. Rumpf, Proc. of SPIE Vol. 10930, 1093012 · © 2019 SPIE
CCC code: 0277-786X/19/$18 · doi: 10.1117/12.2510027

degree of disorder in the photonic nanostructure. Recent work has demonstrated the fabrication of artificial, *Morpho*-inspired nanostructures that exhibit structural coloration effects via a variety of fabrication techniques,[2–4] however prior work has largely neglected the role of tailored disorder in generating iridescence in such bioinspired nanostructures.

These properties emerge from the complex, hierarchical, ridge-like structure abstracted in Figure 1. A key contributor to the fascinating optical properties is the disorder, specifically randomness in height, that is inherent to natural systems. Many researchers have worked on various forms of replication of some or all aspects of this system. However, here we propose and implement an inverse design method with engineered disorder in a physically realizable way.

The characteristic blue color found in *Morpho* butterflies stems from interference within the multi-layer ridge stacks in the chitin.[5] Some elements of this structure can be abstracted out as thin film reflectors, with alternating layers of high and low refractive index.[6] Reflections from these interfaces interfere constructively, and the phase relationship of outgoing waves provides wavelength and angle dependent Bragg conditions.[7] The diffractive effects and high reflectivity of the surfaces arise from the densely packed arrangement of these ridges.[5] Disorder plays a key role in butterfly wings, as the random height offsets between the ridges produce incoherent effects. Removing some coherence of light exiting the structure in turn broadens the output angular spectrum of multi-layer reflection and diffraction. This results in a bright color that appears stable over a wide array of viewing angles. The bright, broad-angle optical effects that make natural photonic systems so captivating often stem from the incorporation of random macroscopic surface elements.[5]

Typically, artificial photonic structures exhibit significantly less disorder than natural systems. Engineered structures are often highly periodic and ordered in a less complex way than living systems.[2] True *Morpho* systems exhibit vibrant colors viewable at wide angle ranges due to the irregularity of their scale structures.[4,8] Material deficiencies (such as low refractive index) that would limit the impact and range of colors are thus mitigated by disorder and irregularity in surface structures.[9]

Unlike with natural structures, producing biomimetic surfaces allows researchers to test beyond tunability that occurs naturally and explore new theory and models to design structures with optimized functions.[10] This process allows us to develop structures with specific intended outputs and properties based on embedded spatial information.[10] The complexity of these structures requires us to employ advanced fabrication strategies that allow for arbitrary three-dimensional structures, which we will discuss further in upcoming sections. In the following section, we outline the design methods used to generate arbitrary structures to create these desired effects.

2. PROBLEM FORMULATION AND DESIGN

In referring to bio-inspired design, researchers can attempt either to mimic the output and spectral response of natural structures, or replicate the structure of the wing itself. Here we focus specifically on mimicking the spectral response of butterfly wings. Instead of mimicking the exact *Morpho*, we produce a structured surface to exhibit a specific color response. In doing so, we are not limited to what is found in nature.[3]

Here we present a comprehensive method for iterative inverse design of a biomimetic *Morpho*-inspired photonic structure exhibiting tailored disorder, and a fabrication methodology based around direct femtosecond laser writing. Our design framework explicitly accounts for the important role of disorder in generating the iridescent effects seen in biological examples of structural coloration. We aim to find a prescribed nanostructure with a prescribed reflectance distribution function, so ultimately we are not limited to existing structures (or colors) found in nature.

$$\hat{h}(x,y) = h(x,y) + n(x,y)\,, \tag{1}$$

Our inverse design method can be described through two components, as described in Equation 1. Here, h represents the height map generated to mimic structural coloration, n represents the height map generated to represent randomness, or "noise," and $\hat{h}$ represents the combined height map generated through this process. We use an iterative design process to optimize a structure based around a desired spectral output to account for

the color output, as described in Sections 2.1-2.4. We then address the second problem of wide viewing angles by engineering a disorder function based on a target power spectral density to replicate the randomness of natural systems, as described in Section 2.5. These two goals ultimately combine into one joint structural height map. In Section 3, we discuss the process of fabricating these structures.

In this optimization process, we compare the forward model of a structure, described in Sections 2.1 and 2.2, to a given reflectance distribution function, which is then optimized in phase space. In this investigation, we rely on abstractions of wide angle diffusion and structural color, but further examination is needed to compare the actual *Morpho* with a multi-layer stack to determine if other optical properties are necessary to achieve the full optical functionality of the butterfly.

2.1 Inverse Design and Goals

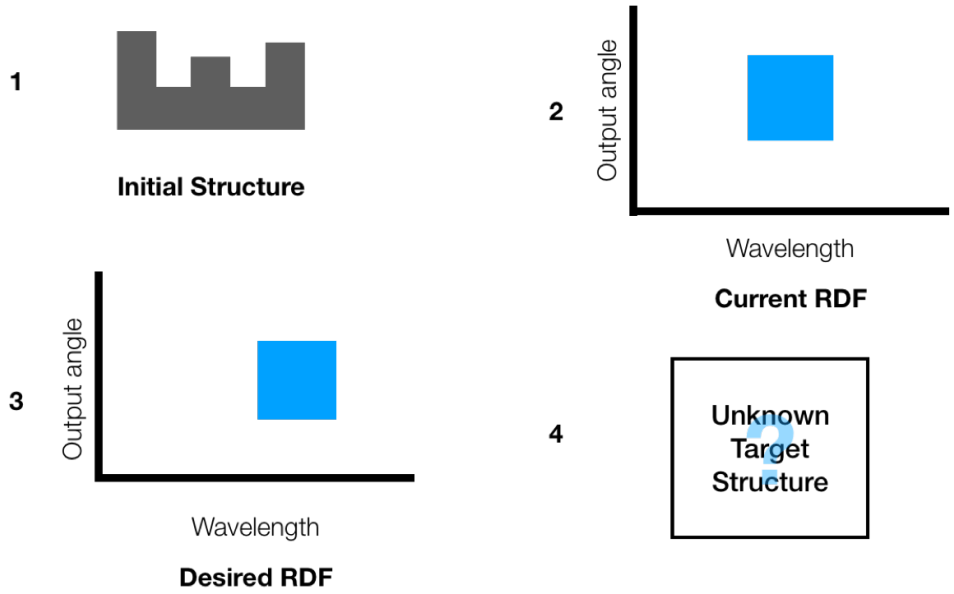

Figure 2. Components of the inverse design process: 1) Initial height map, 2) Reflectance distribution function found using a forward model, 3) Target reflectance distribution function, and 4) unknown target structure.

The first component of the proposed design process is the structure and resultant reflectance distribution function (RDF). We start with the existing *Morpho* structure and examine the structural elements that contribute to desired optical effects. Then, we simplify the structure down to an abstracted form for the purposes of optimization - in this instance arbitrary height maps. We perform a spectral transform on this abstract or simplified structure, and use this process to compute a near field response from the interaction of light with the surface. This near field response is then transferred to a far field response as the viewing perspective will be comparatively far. A RDF is calculated from this spectral transform, providing a metric for evaluating the spectral response of any generated structure. The structure is then perturbed and altered slightly, a new RDF is calculated, and this output is compared to our initial "target" response. Based on the error energy from this new output, the structure is further altered, and the final RDF is confirmed. We then incorporate disorder, evaluate the final response, and incorporate physical fabrication constraints.

This process, thus, has four components (as shown in Figure 2): 1) an initial structure and height map, 2) the current RDF calculated from this structure using the forward model, 3) the target RDF we are iterating towards, and 4) the target structure, which is initially undetermined. The goal is to achieve a specific reflectance spectrum, and during optimization the forward model is used to compare the RDF of the optimized structure to this target. The structure is then updated, the forward model is used to compute a new output, and the iteration of the phase map continues.

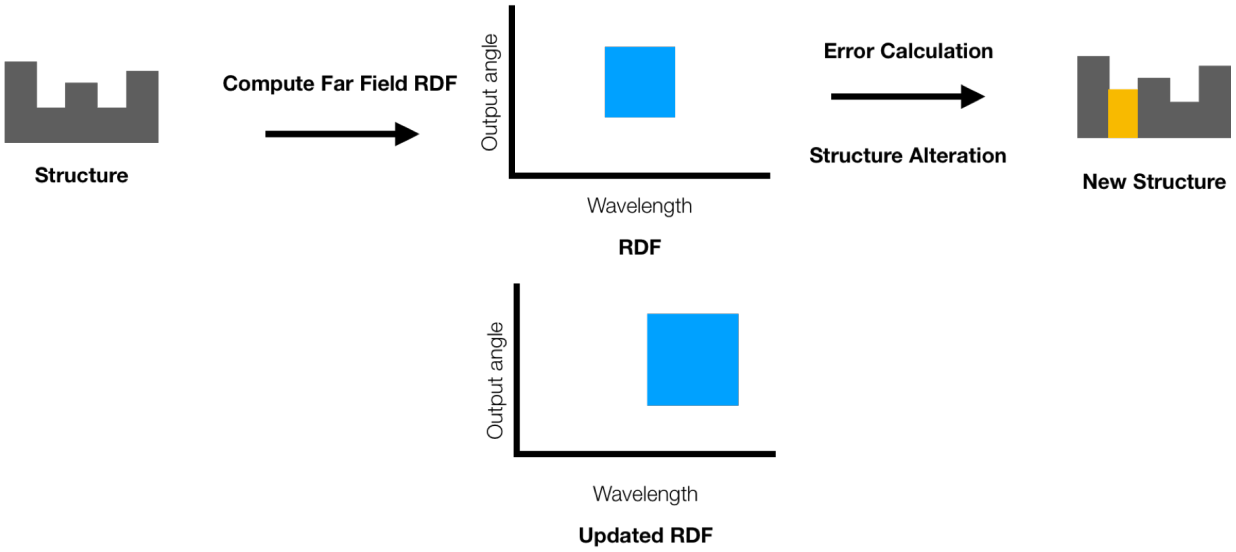

Figure 3. Simplified flow chart of iteration process. Solve the forward model for each input wavelength, integrate into a RDF. This gives a reflectance spectrum of the output, which is the update, and once the update produces the desired output, a structure is generated. The algorithm initially computes a RDF.

2.2 Forward Model and Scalar Diffraction Theory

Often, design of *Morpho*-based systems begins with simulation to optimize performance. Simulations can rely on either analytical or numerical methods, which vary in terms of levels of abstraction. Many numerical electromagnetic and optical approaches have been used to analyze the phenomenon of light scattering from butterfly scale nanostructures.[11] Optical modeling of butterfly or butterfly-inspired structures varies in complexity from more abstract multi-layer stack evaluations to more complex and realistic approaches involving lamellar grating theory or finite-difference time-domain approaches.[12–14]

A frequently used simulation method is the finite difference time domain approach, which can be used to examine the interaction of incoming light with 2-D and 3-D structures and to compute the scattered field off of structures. However, this method is computationally intense and can be time consuming. For our purposes, we rely on a more simplified Scalar Diffraction Theory approach to replicate some aspects of Bragg behavior, described in the following section.[15] This model is widely used for calculating diffraction and surface scattering for applications such as determining reflections emanating from rough surfaces, as it relies on simple mathematical expressions. Thus, it allows for rapid calculations that enable repetitive simulations.

Scalar Diffraction Theory provides computationally simple calculations and thus an accessible starting point for our inquiry, but it has certain limitations due to the level of abstraction. This model does not account for the vectorial nature of light and disregards polarization. Scalar Diffraction Theory only works well for small angles, due to paraxial limitations.

In proceeding with this work beyond this paper, a rigorous comparison of potential physics engines and optical models is necessary. In our exisiting model, the key relationships we rely on are the objective function, a far field to RDF calculation, and measure for diffraction in the far field. Our process is dependent on a forward model based on Scalar Diffraction Theory to model the physical interaction of light with surface structures, as described through Equations 2, 3, and 4. Input parameters include the incoming spectrum, or the amount of each relevant wavelength that is represented in incoming light. The forward model then takes the input structure and turns it into a phase map and an angular term of phase retardance based on incident angle. The resulting structures exhibit multiple heights, so accumulated phase is the difference between the maximum height and the height of given elements, generating a phase difference based on the offset.

$$h(x,y) = \arg\min \sqrt{\sum_{\lambda_i \in \Lambda} \sum_{\theta_x \in \Theta_x} \sum_{\theta_y \in \Theta_y} \left| f_T(\lambda_i, \theta_x, \theta_y) - f(\lambda_i, \theta_x, \theta_y) \right|^2}, \tag{2}$$

Here, λ_i is the incident wavelength, Λ is the space of all wavelengths, θ_x represents the angle in x, and θ_y represents the angle in y. The desired range of angles is represented by $\{\Theta_{x,max}, \Theta_{y,max}\}$. f_T is the target function we move towards, f is the RDF of the current structure, and $h(x,y)$ is the current height map or structure.

Thus, Equation 2 sets up the objective function, which examines the distance between our target function and our current spectral response. We want to minimize this error based on the Froebenius norm of the error energy, which is the statistical distance metric between our target RDF and the optimized RDF. Minimizing this error is the metric for evaluation in our iterative loop.

$$f(\lambda_i, \theta_{in}, \theta_{out}) = \left| U_{o,\lambda_i}(\theta_x, \theta_y; h(x,y))|_{f_x = x/\lambda_i z, f_y = y/\lambda_i z} \right|^2, \tag{3}$$

This equation provides a conversion between the far field and RDF, where, λ_i is the incident wavelength, Λ is the space of all wavelengths, θ_{in} represents the incident angle, and θ_{out} represents the output. U_o is the output field, θ_x represents the angle in x, θ_y represents the angle in y, and $h(x,y)$ is the current height map or structure. This structure is then evaluated at frequencies dictated by the f_x frequency in x and f_y frequency in y, over the z propagation distance.

$$U_{o,\lambda_i}(x,y;h(x,y)) = \frac{e^{jkz}}{j\lambda z} e^{\frac{jk}{\lambda z}(x^2+y^2)} \iint_{-\infty}^{\infty} U_i(x',y') h(x',y') e^{\frac{-j2\pi}{\lambda z}(xx'+yy')} dx' dy', \tag{4}$$

Here U_o is output field over propagation distance z, and U_i is the incident field. x' and y' are spatial coordinates in the input grid, and x, and y are spatial coordinates in the output grid. k represents the wave vector, as defined by $k = \frac{2\pi}{\lambda}$. This allows us to evaluate the angular projection of a scattering media in a far field based on a Fourier transform of the structure. Equation 3 defines a relationship between the RDF and Far Field, and Equation 4 is a light transport operator (for going from structure to output field) using Fraunhofer Diffraction. Together, these equations form the basis for the inverse design process.

2.3 Optimization and Simulated Annealing

Algorithm 1 Inverse Design: Psuedocode for Simulated Annealing for Synthesis of Structural Color

init $h(x,y) = rand(0, h_{max})$, $E_{best} = E(h)$, $T = 0.1 \cdot E_{best}$
for *each iteration* k
  $h' \leftarrow$ flip m random pixels in h
  if $E(h') < E_{best}$
    $h = h'$, $h_{best} = h'$, $E_{best} = E(h')$
  else
    if $exp(-(E(h') - E_{best})/T) > rand(0,1)$
      $h = h'$
    end
  end
  $T = 0.99 \cdot T$
end

The optimization loop operates using Algorithm 1: an iterative loop, where the objective function is calculated based on the error between the desired spectrum and the spectrum from the optimized structure, with a random height map used as an initial guess. This height map serves as a phased array for light interaction. Simulated annealing, shown in Figure 4, is used to run the optimization process as it works to minimize the distance from the target function by simulating atoms undergoing cooling. The algorithm calculates the error of a structure, flips

a pixel at random, and recalculates the error. We specify a rate of cooling that dictates the rate of perturbation as iterations occur.

At higher temperatures, the pixels will be perturbed frequently and error fluctuates significantly, but as the system cools the error converges towards the ideal solution and there is less fluctuation. At the beginning of the optimization, movement is encouraged even if the value of the objective function is temporarily decreased. As the optimization advances, the temperature drops and movement decreases, so perturbations are less likely to occur if they do not minimize error. If the value of a solution is lower after the next iteration, the program accepts it to avoid local minima, but later in the schedule it converges on the solution. If the temperature is high, Boltzmann probability is also high, but as the system cools the probability also lowers. This method is simple to implement, and thus appealing for this application.

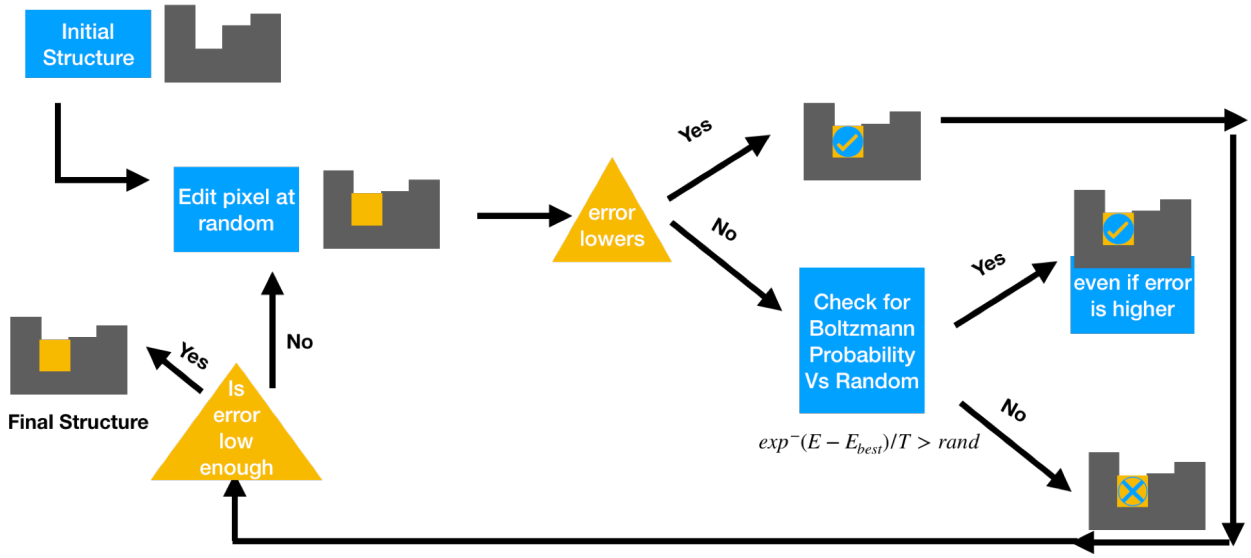

Figure 4. Flow diagram of simulated annealing process. An initial pixel is edited at random. If the error is lower, the change is accepted. The algorithm evaluates the Boltzmann probability, accepts or rejects the change, and determines if the ultimate error is low enough to end the process or continue iterations.

Simulated annealing provides a computationally simplistic and accessible optimization routine for initial investigation, but alternative methods such as gradient-based particle swarm optimization, genetic algorithms, or generative adversarial network-based machine learning techniques should be examined in future work.

2.4 Design Results

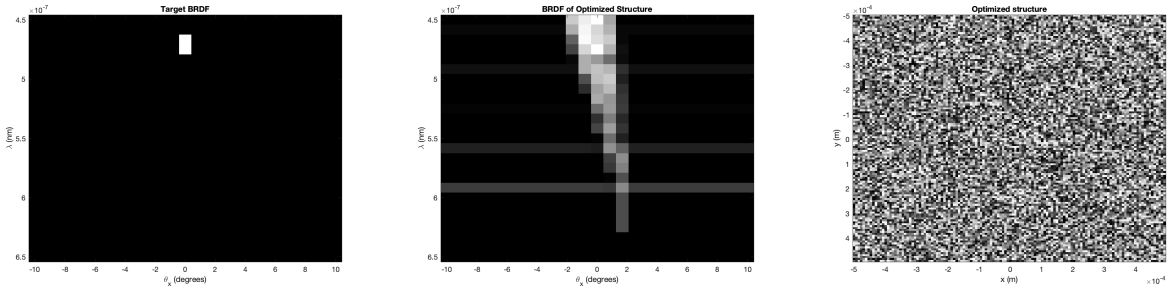

Figure 5. a) Input target RDF defined for our simulations, intended to produce a blue color, b) optical properties (RDF) determined by the iterative solver using simulated annealing, c) generated structure and resulting height map

Here we see the results of a simulation run over 25,000 iterations. The target function in Figure 15a) defines the desired wavelengths and angular distribution: in this case a distribution of wavelengths between 460-480 nm, centered at 473 nm, with an angular spread of 5° and a center angle of 1°. The optimized function, b), shows the resulting spectral response. Further iterations would lead to a more accurate resulting RDF and resulting structure height map. Different grey levels in this map represent different heights between 0 and 5 μm. We then fabricate this using two photon polymerization. These initial structures exhibit specific RDF response, but have no added disorder.

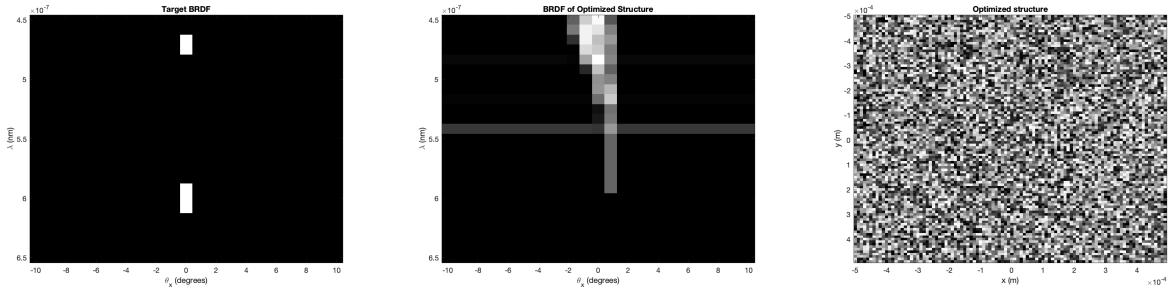

Figure 6. For composite colors based on separate spectral bands our iterative solver has a parallel a) Input target RDF defined for our simulations, intended to produce a two colors, b) optical properties determined by the iterative solver, c) generated structure.

In comparison, for composite coloration we start with two target central wavelengths, each with a spectral bandwidth of 20 nm, as shown in Figure 6. Setting this as a target then allows us to optimize towards a joint RDF that produces both of these color responses, using the same forward model, physics engine, and iterative solver. Thus, we can achieve a composite of two disjoint spectral bands through inverse design methods.

As shown in Figure 6, the RDF achieved through simulatuons is not significantly similar to the target RDF, indicating the need for more complex forward models than Scalar Diffraction Theory. Moving forward, we must compare various physics engines. We propose Helmholtz solvers as a viable and promising alternative.

2.5 Disorder Modeling

Part two of the design we propose, as described by Equation 1, is iridescence: this essentially translates to a wide angle response. Iridescence relies on the addition of a noise term to represent randomness in height to act as a wide angle diffuser. We, thus, need to engineer a noise term with respect to a specific tailored disorder power spectral density. To achieve this, we superpose a noise function that produces a specific power spectral density (PSD) onto the photonic structure engineered through the first simulated annealing optimization loop.

The initial simulated annealing process leads us to a deterministic structure that produces a desired response and engineered structure. We then add an additional optimization loop for the noise function: we use this process to achieve a desired wide angle response from a similar, second random height structure. This disorder function serves to create a diffuser where light spreads out in the manner of the PSD. The engineered disorder function produces a height map that can then be added to the original height map of the structure, ultimately combining these two features as described by Equation 1.

We define the "diffuser function" target power spectral density using Equation 5, which demonstrates the Gaussian distribution used to represent the PSD for the engineered tailor disorder (or noise) function, also shown in Figure 8 . This serves as a Gaussian in angle, where the response is strongest in the center and fades off at higher angles, indicating the manner in which light spreads.

$$P_T(f_x, f_y) = \exp\left(-\left(\frac{f_x^2}{2(\lambda^{-1}\sin(\Theta_{x,max}))^2} + \frac{f_y^2}{2(\lambda^{-1}\sin(\Theta_{x,max}))^2}\right)\right), \tag{5}$$

Here P_T represent the target PSD, f_x, f_y represent frequency terms, and $\{\Theta_{x,max}, \Theta_{y,max}\}$ define the angular range. To produce this tailored disorder noise response, we rely on a Gerchberg-Saxton method for phase retrieval.[16] The noise term exists in the space domain, but we observe the PSD in the Fourier domain. We refer to the linear mapping between angle and frequency, and rely on wavelength dependence. We iterate between the phase and Fourier domain using a ping pong algorithm, as shown in Algorithm 2.

Algorithm 2 Phase Retrieval for Optimized Noise Function: Gerchberg-Saxton Phase Retrieval for Synthesis of Iridescence Noise Function

init $n(x, y) = rand(0, 2\pi)$
for *each iteration* k
  $P = \mathscr{F}(n)^2$
  $P' = P_T e^{j\angle P}$
  $n' = \mathscr{F}^{-1}(P')$
  $n = e^{j\angle n'}$
end

Here, $n(x, y)$ represents the initial noise function, P is the current PSD, P' is the updated PSD, and P_T is the target PSD. F represents the operator for the Fourier Transform, F^{-1} is an inverse Fourier Transform, $\angle P$ is the phase angle of the PSD, and $\angle n$ is the phase angle of the noise function.

Using Algorithm 2, the error around the target PSD and the PSD of the optimized noise function is minimized by use of the Gerchberg-Saxton method for iterative phase retrieval. We maintain the phase of an input noise function after employing a Fourier Transform, but assume the amplitude of a target PSD. We then use an inverse Fourier Transform to get to a new noise function. The loop is demonstrated in Figure 7. The process usually converges rapidly.

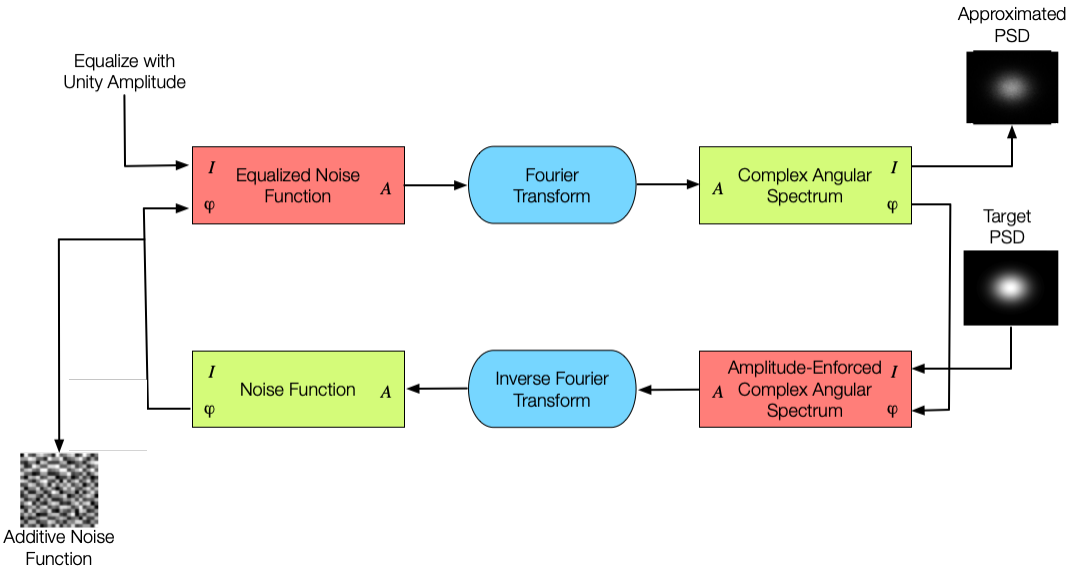

Figure 7. Gerchberg Saxton Algorithm for Phase Retrieval to Produce Noise Function

We can then compare this engineered disorder function to an uncorrelated or random function, as shown in Figure 8. Uncorrelated diffusers should spread light over a greater range of angles, as correlation here implies a small angular spread and lack of correlation implies wide angular spread. In this manner, engineering the noise function in a tailored fashion provides an additional degree of control over the optical functionality and output of our simulated structures. We describe this disorder function further in Section 4.1.

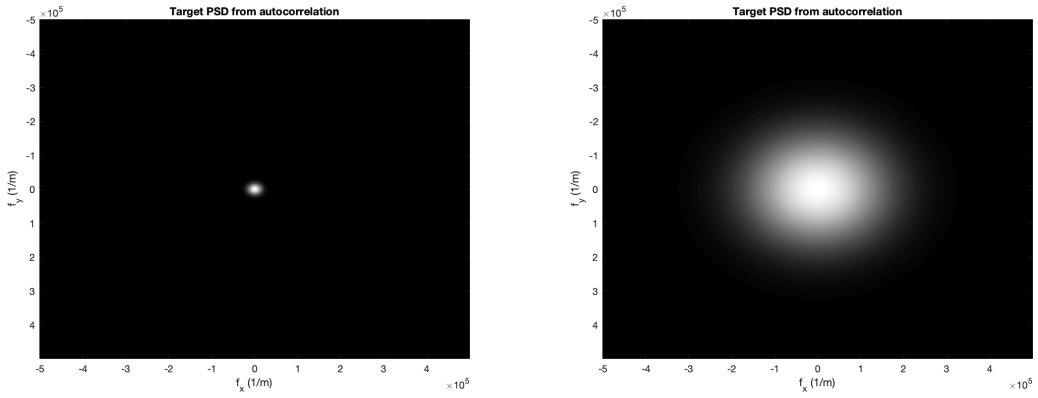

Figure 8. PSD plots for Correlated (left) vs. Uncorrelated (right) additive Disorder Functions, demonstrating a much larger angular spread in the uncorrelated (or more random) diffuser

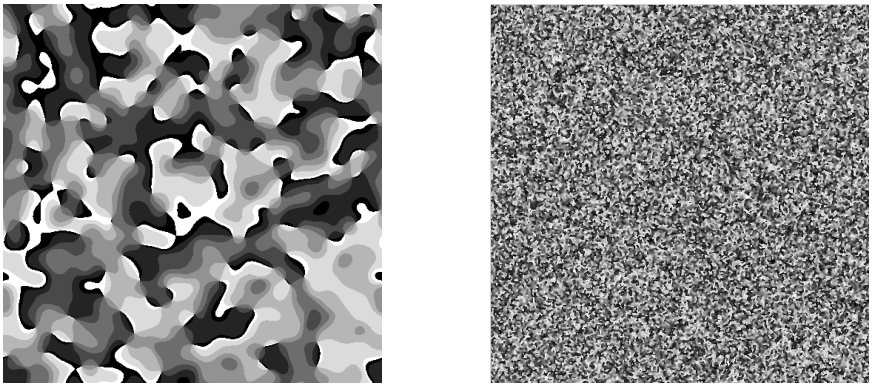

Figure 9. Optimized noise function representing a large correlation (left) and a more random function (right) These images are initial height maps that can then be printed.

We demonstrated successful fabrication of engineered disorder functions using two-photon polymerization, as will be discussed in Section 5 below. While extensive characterization is needed, initial results are promising, as shown in Figure 10.

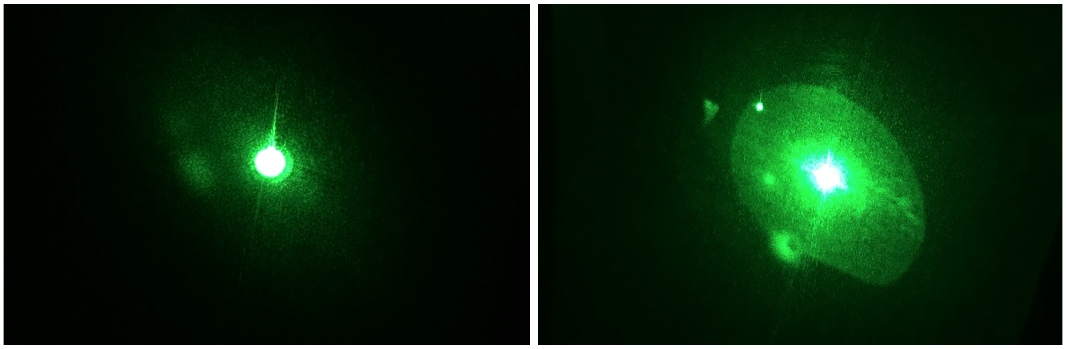

Figure 10. Initial characterization of correlated (left) and uncorrelated (right) diffuser functionality as printed using two-photon polymerization

3. FABRICATION METHODS

3.1 Existing Methods

Complex biologically-inspired systems require advanced fabrication techniques, and replication of nanoscale features of this complexity has been difficult. Existing methods include multi-step deposition, etching, and assembly processes.[11] In comparison to existing fabrication methods for *Morpho*-inspired structures, such as interference lithography, colloidal self-assembly, sputtering, atomic layer deposition, or electron beam lithography,[11] direct laser writing methods allow for flexible, three-dimensional, volumetric feature patterning on multiple length scales.

As the mechanical design of the butterfly wing is quite complex, it can be extremely costly and difficult to fabricate similarly intricate structures. To decrease the associated costs and challenges, researchers often use existing wings as a physical template and coat new materials on top. By specifically relying on dielectric materials for this, photonically active structures can be produced cheaply and easily. Techniques used for templating include atomic layer deposition, physical vapor deposition, and chemical solution deposition.

Additionally, many fabrication methods have been developed for free-form creation of biomimetic structures. Atomic layer deposition is also used to produce multilayer stacks towards bio-inspired structures and generating structures that replicate the hierarchical structure of *Morpho* scale. Additional techniques include lithographic methods like electron beam lithography, soft lithography, nanocasting lithography, nanoimprint lithography, and laser interference lithography. In contrast, fabrication strategies like femtosecond laser patterning, electroforming, and deposition can be used to create irregular patterns in multiple dimensions. This proves extremely valuable for prototyping structures, especially for inverse design methods.

3.2 Ultrafast Direct Laser Material Processing

Ultrafast laser micromachining has emerged as a powerful tool for structural fabrication across many disciplines. The use of femtosecond laser direct writing allows for the rapid prototyping of complex, hierarchical micro- and nano-structures.[17] Laser processing can be used to create integrated device features and arbitrary volumetric structures in a simple and controllable manner, without the use of expensive and restrictive cleanroom equipment. Femtosecond lasers can be used in ambient laboratory conditions, and produce robust, air-stable features structures.[17] The repetition rate of the laser and speed of the stage are primary limiting factors for speed of patterning processes. As a result, femtosecond methods can be much faster than some traditional methods for lithography and etching.

Femtosecond lasers provide a very versatile tool capable of both surface and volume modification due to multi-photon absorption. Achievable processes for the surface of materials include ablation, drilling, micromachining, deposition, and micro- and nano- patterning.[17–19] In transparent materials, volume modification can also be harnessed: including index modification, multi-photon polymerization, and densification processes.[18] Ablative processes allow users to remove material in controlled areas, deposition transfers material from one substrate to another, and densification is used to alter material refractive indices.[17]

As such, laser processing can be used achieve multiple processes in one tool, replacing extensive cleanroom processing and providing a platform for integrated device fabrication. Two key features of ultrafast laser processing that enable unique capabilities are spatial and temporal confinement. The speed of pulses allows for temporal confinement as it can surpass the speed of heat diffusion in a material. The processes depend on nonlinear effects from electron excitation of a localized spot, so above a certain threshold ablation occurs straight from a solid to a plasma without going through a liquid phase, allowing from higher resolution writes. Material interactions with femtosecond pulses occur on a quick enough timescale that thermal effects can be ignored.[19] Spatial confinement of the laser beam interaction region and focal volume similarly allows for high resolution features. Ellipsoidal voxels serve as the basic building block for these processes as intensity decreases rapidly in a Gaussian fashion for the x and y dimensions, but not the z dimension.[19]

For this specific biomimetic process, two-photon polymerization is the most effective fabrication method. When combined with the design and optimization process presented here, this method allows for the use of the *Morpho* structure as a baseline for iteration, both to incorporate tailored disorder, and to produce structures with extended functionality beyond existing systems. In doing so, we present a versatile approach to bio-inspired

materials design and and provide a platform with applications ranging from light harvesting and steering, to chemical sensing, high performance displays, responsive products and architecture. Two-photon polymerization and other direct laser writing techniques provide amenable platforms for rapid prototyping of simulated optimized structure to test for practical fabrication and implementation that provides a cost- and time-effective alternative to traditional lithographic methods. These evaluated and characterized structures can then be adapted to roll to roll or imprint based systems for scale-up and manufacturing on a commercial scale.

3.2.1 Two-Photon Polymerization

To develop a flexible fabrication method to analyze color formation based on hierarchical structures with disorder, proper integration of micro- and nano-structures must be achieved. In contrast to other lithography methods, two-photon polymerization offers this flexibility due to the maskless fabrication of arbitrary structure shapes and its simple production process.

Two-photon polymerization processes use a chain polymerization reaction that causes a resist to solidify in the focus region of the laser beam, acting as an additive manufacturing process. In this manner, the tool can be used to write a three-dimensional structure in the volume of the material as the beam rasters through. As it allows for arbitrary three-dimensional structures, this technique is more versatile than traditional etching and lithography methods.

Two-photon polymerization is a nonlinear process through which intensity scales with absorption squared. For two-photon polymerization, absorbed intensity scales with squared laser intensity. Polymerization is limited to the focus area of the beam, as variable pulse energy is controlled to exceed the polymerization threshold in that region. The intensity of the beam follows a Gaussian distribution, and intensity decreases rapidly as distance from the focus region increases. This effect is much more prominent in multi-photon processes than single-photon processes. Optimal photoresists appear transparent to the beam based on the single-photon energy threshold as compared to the absorption properties of the material. However, in the focus region of the laser beam, multi-photon phenomena achieve a high enough intensity to surpass the threshold and expose the resist.[20]

3.2.2 Two-Photon Polymerization Using the Nanoscribe GmbH System

Typically, two-photon polymerization processes rely on photosensitive resins, specifically acrylic-based materials, where many researchers rely on resists such as SU-8.[21] Two-photon fabrication uses a photoinitator to trigger a reaction in the base resin material. For positive resists, as the laser interacts with the material, radicals are generated, which then react with the polymer to form high molecular weight materials through chain growth reactions.[21] For acrylics, the chain addition occurs in the carbon-carbon double bond in the ester moeities.[21] The double bonds decrease as new carbon-carbon bonds form.[21] In this reaction, the initial monomer form is a low-energy state, and the polymerized material is a high energy state.[22] A commercial option for two-photon

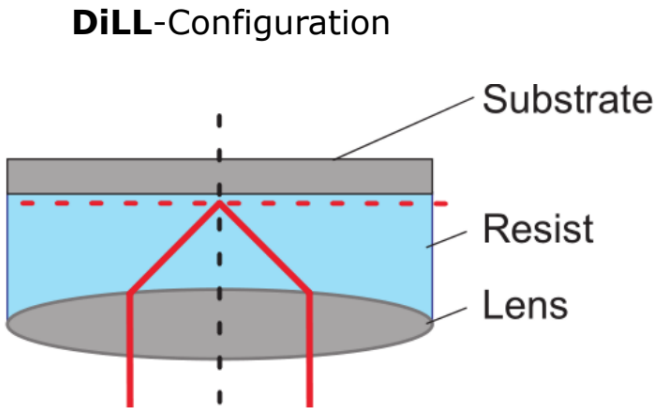

Figure 11. Dip-in Laser Lithography for two-photon polymerization with Nanoscribe[23]

processing is the Photonics Professional by Nanoscribe GmbH system, which can achieve features down to 100 nm. For this system, a piezoelectric motor is used to move the laser, rather than the stage. The system uses continuous writing where the laser is continuously on. Multiple configurations can be used, but a commonly used mode is the Dip-in Laser Lithography (DiLL) mode where the microscope objective is directly dipped into the photoresist. The resist is placed upside down and the objective points up into the liquid, where the resist itself is used as the immersion fluid for the lens. Dipping the lens directly into the resist limits spherical aberrations and allows for non-transparent substrates for the material. The maximum structure height is limited by the sample holder used and may be larger than 2 mm. This allows for mesoscale features that combine sub-micron resolution with large-area prints.[24] Users alter the ellipsoidal voxel size by varying the laser power, but height is minimally one micron. Fused silica is the most commonly used substrate for Nanoscribe prints, with a refractive index of n = 1.46. Nanoscribe produces resists specifically for the system, and a commonly used negative-tone resist is IP-DIP (Nanoscribe GmbH): an acrylic material that is transparent in the visible spectrum and has a refractive index of n = 1.52. In order for the focus process of the system to work, the resist must have a sufficiently different refractive index from the substrate, typically of at least 0.05. The beam operates at 780 nm, with a pulse duration of 100 fs and a repetition rate of 80 MHz. Multiple objectives can be used, but here we used a 63X objective with NA 1.4. All Nanoscribe writes begin with an automatic interface-location procedure to ensure that the print adheres to the substrate through some overlap. Focusing inside the solid substrate has no negative impacts on the substrate, but does ensure that the structure will stick effectively. If the intensity of the beam is too low, adequate solidification will not occur and the structure may not withstand development. After the write process, the resist is developed and all but the solidified region is washed away using Propylene glycol monomethyl ether acetate (BTS-220 by Baker).

4. PRELIMINARY RESULTS

4.1 Structurally Colored Surfaces and Additive Disorder Functions

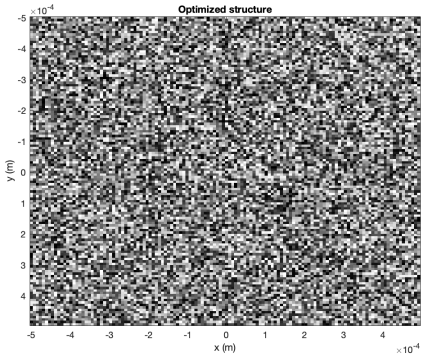

Figure 12. Optimized height map resulting from simulated annealing simulations. Grey-levels in this output image indicate the height of the feature to be printed, ultimately resulting in an arbitrary three-dimensional print with a desired optical response.

Here we demonstrate multiple prints of both simulated structures and diffusers to indicate an effective work-flow that enables the robust fabrication of samples based on the iterative solver. While a variety of write parameters for the IP-Dip resist were examined, the fabricated samples shown here were written at 100% laser power, and 40mm/s scan speed. We characterized satisfactory replication of simulated grey-level height maps, indicating the viability of this process. Thus far, our samples have primarily been characterized using SEM analysis.

Both the correlated and uncorrelated diffusers were effectively printed and robustly reproduced the intended simulated result. The structure of the correlated and uncorrelated noise functions are evidently extremely different, leading to very different diffusion behavior. Further characterization is needed to rigorously demonstrate this behavior. Ultimately, the height profiles generated for such noise functions would be combined with the

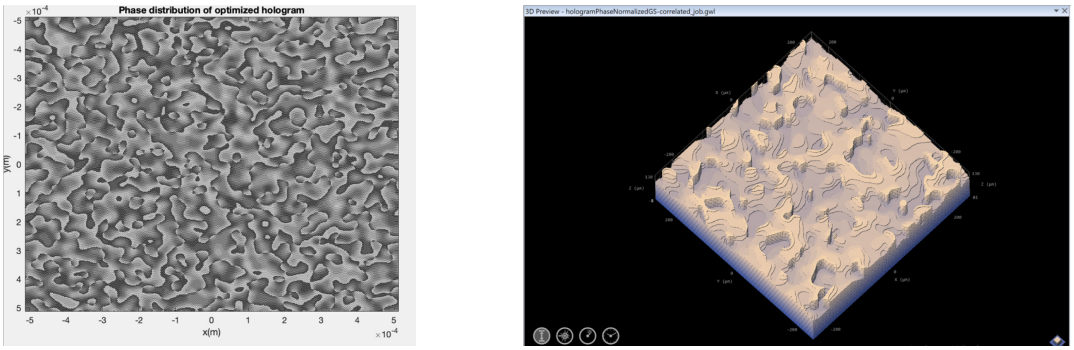

Figure 13. The additive disorder function was simulated as explained in the sections above, resulting in the grey-level image on the left. This image was then imported into the DeScribe software environment to prepare it for fabrication, as demonstrated on the right. As shown here, the simulated results can be reproduced effectively in physical form using this system.

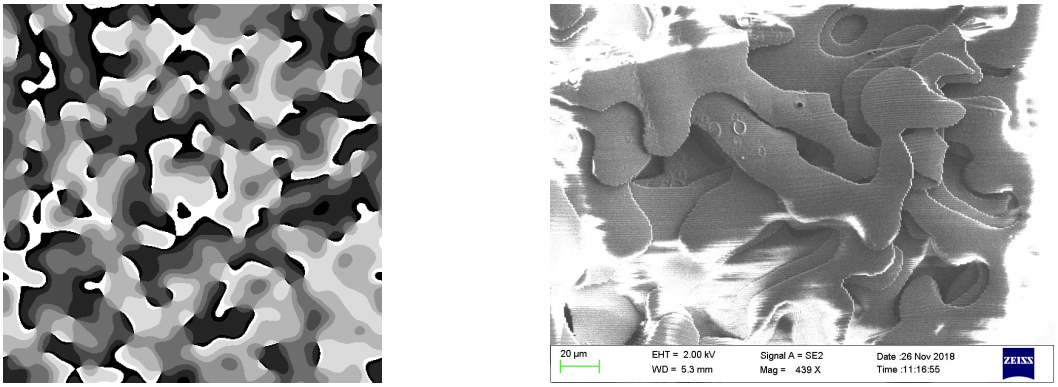

Figure 14. A) Optimized Disorder Function for Tailored Noise Function B) SEM of Fabricated Disorder Function: Correlated (Based on a Target PSD) This is an engineered diffuser with a target PSD angular distribution.

optimized structure height map to produce a final simulated structure that we would then fabricate to combine both color and wide angle diffusion properties, effectively mimicking the *Morpho*. Proper combination of these features would need to occur via phase addition (by considering retardance of phase, rather than pure height) to maintain the full dynamic range.

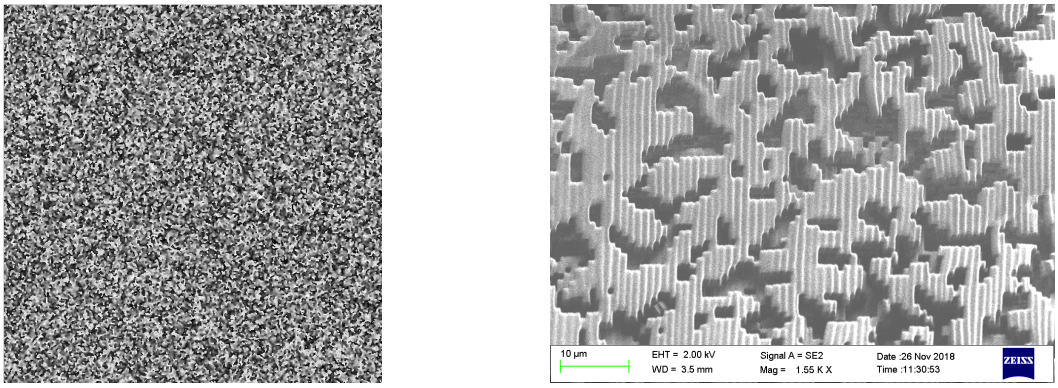

Figure 15. A) Simulated Disorder Function for Uncorrelated Noise Function B) SEM of Fabricated Disorder Function: Uncorrelated (Random).

While these samples demonstrate the foundation needed to develop the proposed method, further work is needed to optimize cleaning and preparation of the substrate surface to promote adhesion. Additionally, further parameter sweeps are needed to optimize dose and scan speed for each of these optical structure types. Polymerization processes are optimized using voxel by voxel testing as the experimenter varies laser power and write speed to alter the fluence of the system.

4.2 Nanoscribe Prints of Other Model Optical Elements

In the process of developing an effective workflow and ensuring that our optimization scheme produces physically realizable features that are compatible with the Nanoscribe system, we tested a variety of prints of optical elements, including phase holograms and diffraction gratings and shown in Figure 16 and Figure 17. Ultimately, these features could be combined with generated height maps and other aspects of biomimetic structures to create multi-element, multi-layered systems that better imitate the interplay between structures in existing butterfly wings.

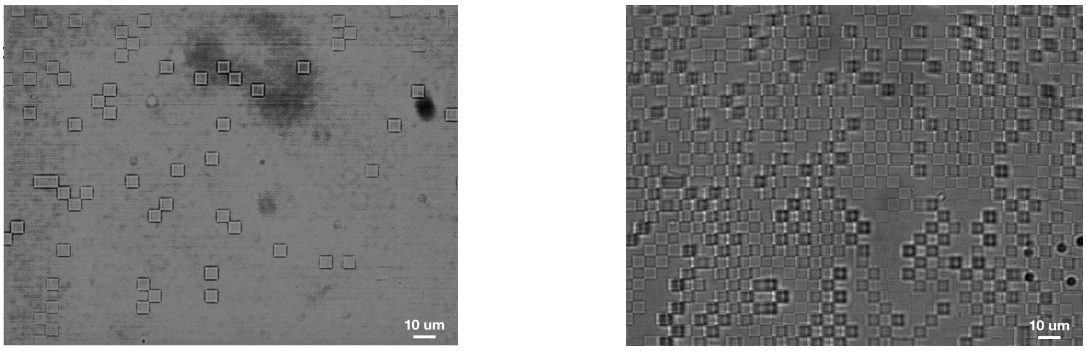

Figure 16. SEM images of pixels written using Nanoscribe system, demonstrating grey-level conversion to different pixel heights towards arbitrary height maps

Through these initial writes, pixels of different heights are clearly visible, as shown in Figure 16, indicating an effective mapping of grey-level images to printable elements. Further characterization is needed to define the full range of printable heights using the current image to print process, but phase hologram writes are a promising start. Similarly, Figure 17 demonstrates a regular, functional diffraction grating written over a relatively large area. We have confirmed that two-photon polymerization is a viable and convenient process to test our simulated results, and write times are reasonable for these structures.

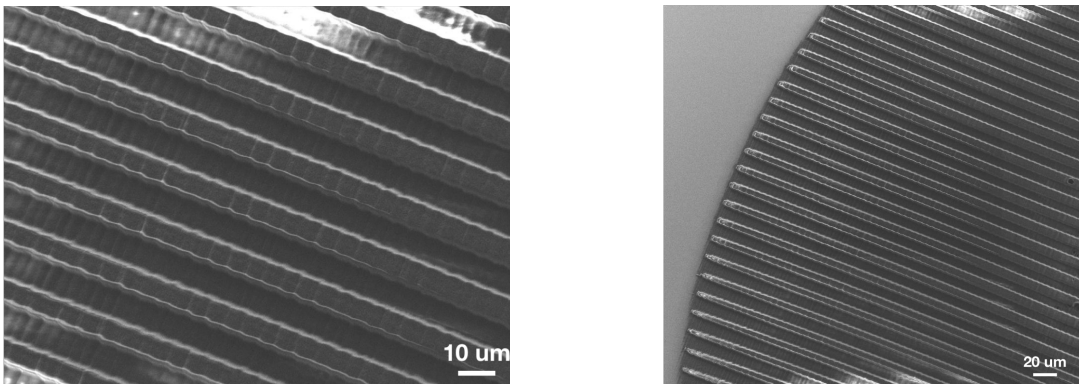

Figure 17. Grating Written Using Two-Photon Polymerization

5. DISCUSSION AND CONCLUSIONS

In this paper we have outlined and tested an iterative inverse design method that can be used to mimic the optical function of *Morpho* butterfly wings by optimizing towards a target RDF with an additional noise term in a physically realizable manner. We further demonstrated that this noise term can also be engineered towards a target power spectral density to mimic the functional impact of randomness found in natural structures. Our primary contributions are as follows: application of Scalar Diffraction Theory for a forward model, demonstration of an iterative algorithm for optimizing the optical structure using inverse design to produce a desired spectral response, confirmation that two-photon polymerization is a viable process, development of correlated and uncorrelated disorder functions for representing randomness and iridescence, and creation of a workflow to enable writes.

While this paper outlines the methods and theory needed to engineer desired optical responses, based on the conclusions we have demonstrated, we will continue to fabricate and characterize samples to ensure that the physical constraints and models produce realizable, functional structures. We aim to compare our model system and simulations to fabricated structures using optical microscopy, scanning electron microscopy, and angular spectrometry. Developing a further understanding of the achievable depth and height profiles of current prints using existing doses will allow us to achieve higher resolution, more robust surface profiles.

In parallel, we will continue to develop effective models for simulating light-surface interactions, while maintaining simple calculations that reduce computational load. While immediate goals include comparison between vectorial wave solving methods (using Helmholtz solvers), additional measures could address multiple pixels at once during optimization routines. One method for addressing this would be to examine the role of tiled motifs to represent the disorder factor present in natural systems. Using a motif would allow us to focus on a small region and repeat this unit over the entire surface, simplifying calculations.

In addition to considering new forward models and physics engines, we must also examine alternatives to simulated annealing for the optimization routine. Initial options include genetic algorithms, generative adversarial networks, or gradient descent methods to update multiple pixels in specific patterns.

Furthermore, future efforts may examine deeper and more complex volume elements in addition to surface patterns. Using surface profiles as the only means of directing light only provides one opportunity to reflect light, whereas volume elements allow for the development of higher intensity features. Adding mirror layers or volume elements (multi-layer stack with surface elements) allows for more light from reflection than are achievable from pure refractive index changes.

More broadly, the benefits of such biomimetic nanostructures are plentiful: they provide brilliant, iridescent color with mechanical stability and light steering capabilities. The colors do not fade over time in the manner that traditional pigments do. Biomimetic structurally colored surfaces have many features that make them interesting for consumer devices and products. Structural color can be harnessed for long-lasting paints, fabrics, and displays.[25] The wing structures have interesting surface properties, such as hydrophobic behavior, that are both functional and compelling. By producing biomimetic nanostructures, designers and engineers can capitalize on unique properties of optical structural color, and examine these structures based on human perception and response. The color changes achievable with these structures are intuitively interpretable by humans, providing some fascinating use cases.[10] Applications include vapor-based environmental and chemical sensing: the structures visually change color as certain volatile substances adhere to the surfaces. This color change could serve as a rapid visual sensor for environmental agents, providing an easy means for individuals to understand a bit more about their local environments. These techniques can be applied towards color changing strain sensors and interfaces, and the optical modeling and metamaterial fabrication principles can be applied towards precise light steering applications like optical resonators or solar cell concentrators.[10] Drawing from transparent systems like the glasswing butterfly could further move us towards systems that camouflage and entirely cloak elements and move towards invisibility cloaks.

The processing methods we rely on here will allow researchers to produce integrated devices in which biomimetic structures are combined with electrically active elements and other functional pieces. Building off of these design methods, we hope to incorporate modeling of mechanical properties in order to iteratively optimize material properties for desired perceptual responses. We can then move towards active surfaces that

produce one spectral response in one mechanical configuration and a different mechanical configuration in a second configuration using joint optimization methods. By combining the sensing modalities with responsive mechanical properties, we can examine dynamically tunable and environmentally responsive structural color.

Typically, dynamic response relies on one of three mechanisms: 1) a change in refractive index, 2) change in spacing of periodic structure or 3) change of direction of illumination. For instance, cephalopod structures control the thickness of their protein platelets using swelling, or by altering the spacing between these platelets. They are able to tilt these platelets to alter the manner in which incident light interacts with the surface and the wavelength of selective reflection.[26] In multi-layer stacks similar to the *Morpho* design, we can alter and tune color by altering the distance between stacks, or by altering the refractive index of the material. Producing structurally colored surfaces on more flexible substrates will allow us to examine mechanical responses. Ultimately, we hope combine composite and multiplexed systems with concepts of active and dynamic coloration.

As mentioned above, femtosecond processes provide an accessible, cost-efficient method for prototyping quickly based on optimized structures, before processes are moved to roll to roll or imprint systems. Beyond the manufacturing implications, this work can ultimately have some beneficial outcomes from a sustainability perspective. Structural colors are known for being robust, mechanically durable, and long-lasting: moving away from traditional pigments and towards longer-lasting, UV-resistant colors could allow us to develop more durable paints with a longer life cycle. If this application is coupled with the potential for an eco-friendly production process that can be applied to a broader array of materials, we could harness greener coloration processes. Finally, as mentioned in the introduction, understanding the methods used to generate specific spectral outputs will allow us to create colors we cannot currently achieve in nature, especially as combined with dyanmic, mechanically adaptive systems or printable, integrated devices.

ACKNOWLEDGMENTS

This research has been supported by consortium funding at the MIT Media Laboratory. The authors gratefully acknowledge facility use and technical assistance by the MIT Nanostructures Laboratory, Harvard Center for Nanoscale Systems and the MIT Center for Bits and Atoms. In particular, we thank Jim Daley, Mark Mondol, Guixiong Zhong, Mathias Kolle, Will Langford, Prashant Patil, Sunanda Sharma, Nick Schneider, and Nick Savidis for their technical support and contributions, and Pedro Colon-Hernandez, Colleen Reynolds, and Michael Wallace for broader support.

REFERENCES

[1] Saito, A., Yonezawa, M., Murase, J., Juodkazis, S., Mizeikis, V., Akai-Kasaya, M., and Kuwahara, Y., "Numerical analysis on the optical role of nano-randomness on the morpho butterfly's scale," *J. Nanosci. Nanotechnol.* **11**, 2785–2792 (Apr. 2011).

[2] Zyla, G., Kovalev, A., Grafen, M., Gurevich, E. L., Esen, C., Ostendorf, A., and Gorb, S., "Generation of bioinspired structural colors via two-photon polymerization," *Scientific reports* **7**(1), 17622 (2017).

[3] Andkjær, J., Johansen, V. E., Friis, K. S., and Sigmund, O., "Inverse design of nanostructured surfaces for color effects," *JOSA B* **31**(1), 164–174 (2014).

[4] Vukusic, P., Sambles, J., Lawrence, C., and Wootton, R., "Quantified interference and diffraction in single morpho butterfly scales," *Proceedings of the Royal Society of London B: Biological Sciences* **266**(1427), 1403–1411 (1999).

[5] Song, B., Eom, S. C., and Shin, J. H., "Disorder and broad-angle iridescence from morpho-inspired structures," *Optics Express* **22**(16), 19386–19400 (2014).

[6] Rayleigh, L., "Xxvi. on the remarkable phenomenon of crystalline reflexion described by prof. stokes," *The London, Edinburgh, and Dublin Philosophical Magazine and Journal of Science* **26**(160), 256–265 (1888).

[7] Vukusic, P., Sambles, R., Lawrence, C., and Wakely, G., "Sculpted-multilayer optical effects in two species of papilio butterfly," *Applied optics* **40**(7), 1116–1125 (2001).

[8] Kinoshita, S., Yoshioka, S., and Kawagoe, K., "Mechanisms of structural colour in the morpho butterfly: cooperation of regularity and irregularity in an iridescent scale," *Proceedings of the Royal Society of London B: Biological Sciences* **269**(1499), 1417–1421 (2002).

[9] Zollfrank, C., "Bioinspired material surfaces–science or engineering?," *Scripta Materialia* **74**, 3–8 (2014).
[10] Steindorfer, M. A., Schmidt, V., Belegratis, M., Stadlober, B., and Krenn, J. R., "Detailed simulation of structural color generation inspired by the morpho butterfly," *Optics Express* **20**(19), 21485–21494 (2012).
[11] Butt, H., Yetisen, A. K., Mistry, D., Khan, S. A., Hassan, M. U., and Yun, S. H., "Morpho butterfly-inspired nanostructures," *Advanced Optical Materials* **4**(4), 497–504 (2016).
[12] Botten, L., Craig, M., McPhedran, R., Adams, J., and Andrewartha, J., "The finitely conducting lamellar diffraction grating," *Optica Acta: International Journal of Optics* **28**(8), 1087–1102 (1981).
[13] Li, L., "A modal analysis of lamellar diffraction gratings in conical mountings," *Journal of Modern Optics* **40**(4), 553–573 (1993).
[14] Plattner, L., "Optical properties of the scales of morpho rhetenor butterflies: theoretical and experimental investigation of the back-scattering of light in the visible spectrum," *Journal of the Royal Society Interface* **1**(1), 49–59 (2004).
[15] Johansen, V. E., Andkjær, J., and Sigmund, O., "Design of structurally colored surfaces based on scalar diffraction theory," *JOSA B* **31**(2), 207–217 (2014).
[16] Gerchberg, R. W., "A practical algorithm for the determination of phase from image and diffraction plane pictures," *Optik* **35**, 237–246 (1972).
[17] Datta, B. C., Savidis, N., Moebius, M., Jolly, S., Mazur, E., and Bove, V. M., "Direct-laser metal writing of surface acoustic wave transducers for integrated-optic spatial light modulators in lithium niobate," in [*Advanced Fabrication Technologies for Micro/Nano Optics and Photonics X*], **10115**, 101150W, International Society for Optics and Photonics (2017).
[18] Sugioka, K. and Cheng, Y., "Ultrafast lasers—reliable tools for advanced materials processing," *Light: Science &Amp; Applications* **3**, e149 (Apr. 2014).
[19] Savidis, N., Jolly, S., Datta, B., Karydis, T., and Bove, V. M., "Fabrication of waveguide spatial light modulators via femtosecond laser micromachining," in [*Advanced Fabrication Technologies for Micro/Nano Optics and Photonics IX*], **9759**, 97590R, International Society for Optics and Photonics (2016).
[20] Anscombe, N., "Direct laser writing," (2010).
[21] Xiong, W., Jiang, L., Baldacchini, T., and Lu, Y., "Laser additive manufacturing using nanofabrication by integrated two-photon polymerization and multiphoton ablation," in [*Laser Additive Manufacturing*], 237–256, Elsevier (2017).
[22] Stolte, E. et al., *Characterisation of 3D-printed micro-structures for optics*, B.S. thesis (2018).
[23] "3D micro-printing by direct laser writing." https://www.nanoscribe.de/.
[24] Bückmann, T., Stenger, N., Kadic, M., Kaschke, J., Frölich, A., Kennerknecht, T., Eberl, C., Thiel, M., and Wegener, M., "Tailored 3d mechanical metamaterials made by dip-in direct-laser-writing optical lithography," *Advanced Materials* **24**(20), 2710–2714 (2012).
[25] Vukusic, P. and Sambles, J. R., "Photonic structures in biology," *Nature* **424**(6950), 852 (2003).
[26] Dushkina, N. and Lakhtakia, A., [*Engineered Biomimicry: Chapter 11. Structural Colors*], Elsevier Inc. Chapters (2013).